The final results of the integral emissivity calculations for polyethylene and polyethylene terephthalate are presented in Table 1. The following values of reflection coefficient R^* were used in the calculations: polyethylene, 0.08; polyethylene terephthalate, 0.12.

It is evident from Table 1 that with increase in temperature the emissivity of the polyethylene film, calculated with the above assumptions, increases, while $\varepsilon(T)$ of the terephthalate film first increases, then falls. This is because with increase in temperature the maximum of the Planck radiation for the polyethylene film moves into a spectral region where transmission decreases. The polyethylene terephthalate transmission spectrum is more "broken," so that the temperature dependence of its emissivity is more complex in character.

LITERATURE CITED

1. M. A. Bramson, Infrared Radiation, Plenum Publ. (1968).
2. S. G. Il'yasov and V. V. Krasnikov, Inzh.-Fiz. Zh., 19, No. 5 (1970).
3. D. B. Adamov, M. B. Pankova, A. I. Petrov, and V. S. Savinich, Questions of Radio Electronics, General Technical Series [in Russian], No. 11 (1975), p. 80.

ELECTRODIFFUSION ANEMOMETRY OF POLYMER SOLUTIONS

N. A. Pokryvailo, A. S. Sobolevskii, Z. P. Shul'man, and T. V. Yushkina

UDC 532.135:532.522

Theoretical and experimental studies are reported for the convective diffusion occurring at the electrode of an electrodiffusion anemometer, particularly with regard to the measurement of average and fluctuation velocities in rheologically complex liquids and weak polymer solutions.

Information on the velocity pattern in laminar or turbulent flow is of decisive importance in research on convective heat and mass transfer. The thermoanemometer method may be applied to rheologically complex liquids, which may have various properties: viscoelasticity, pseudoplasticity, viscoplasticity, mechanodestruction, and thermodestruction, which involves various difficulties. In particular, there is a marked fall in sensitivity in measurements on polymer solutions of WSR-301 type [1, 2] and also the occurrence of anomalous signals unrelated to turbulent velocity fluctuations [3]. Very promising methods such as laser anemometry [4, 5] and other optical methods become largely unsuitable if the fluid is opaque or strongly scattering. It is also of little value to use Pitot tubes with piezoelectric conversion at low speeds, although they can be used to measure velocity fluctuations in turbulent flows of polymer solutions in pipes [6] and enclosed jets [4, 7].

Electrochemical measurement of velocity has some major advantages such as high sensitivity, long working life in the electrodes, comparative simplicity in the equipment, and scope for using the transducer for several purposes [8, 9, 13, 19].

The theory and practice of the electrodiffusion anemometer have been considered [10, 11], particularly when the sensitive surface is a continuous cone or wedge. Such an electrode can be used with a nonlinearly viscous power-law liquid in the following rheological equation of state:

$$\tau = k\left|\frac{\partial u}{\partial y}\right|^{n-1}\frac{\partial u}{\partial y} \tag{1}$$

and the equation for convective diffusion can be solved analytically to give expressions for the static and dynamic characteristics [10, 11].

The solution to

$$u\frac{\partial c}{\partial x} + v\frac{\partial c}{\partial y} = D\frac{\partial^2 c}{\partial y^2} \tag{2}$$

Lykov Institute of Heat and Mass Transfer, Academy of Sciences of the Belorussian SSR, Minsk.

Translated from Inzhenerno-Fizicheskii Zhurnal, Vol. 37, No. 2, pp. 289-298, August, 1979. Original article submitted July 4, 1978.

0022-0841/79/3702-0943 $07.50

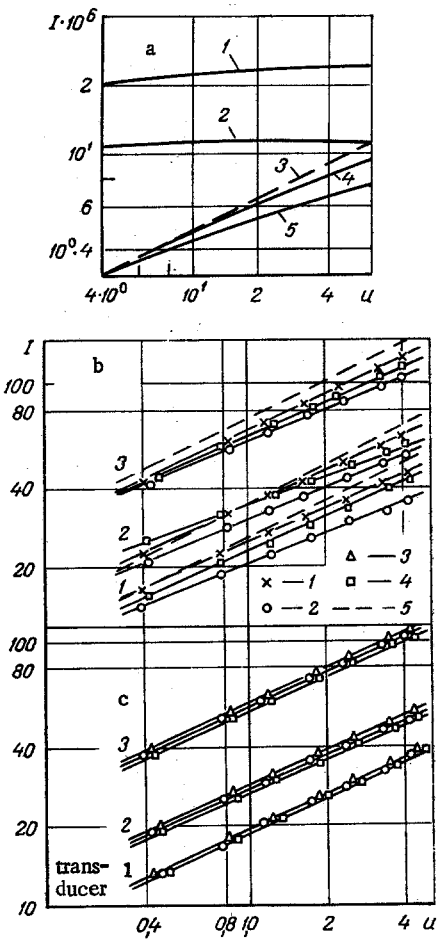

Fig. 1. Diffusion current I (μA) as a function of speed u (m/sec): a) calculation of the effect from the finite electrochemical reaction rate [1, 2) Pr = 10, $k_1 = 10^{-3}$, $5 \cdot 10^{-4}$ m/sec; 3, 4, 5) Pr = 10^3, $k_1 = \infty$, 10^{-3}, $5 \cdot 10^{-4}$ m/sec, respectively]; b) calibration in pure electrolyte (1) and in PEO solutions [2) 0.05%, 4) 0.003%, 5) from theory]; c) calibration in Na-CMC solutions [2) 0.05%; 3) 0.01%; 4) 0.003%].

subject to the boundary conditions

$$c(x, \infty) = c_0; \quad c(0, y) = c_0; \quad D \left.\frac{\partial c}{\partial y}\right|_{y=0} = k_1 c(x, 0), \tag{3}$$

corresponding to a finite rate of electrochemical reaction at the surface reveals the effects from the shape of the body, the value of k_1, and the properties of the liquid [10].

Figure 1a shows the diffusion flux in relation to velocity [10], and it is clear that the sensitivity of a device working with Pr = 10 is substantially less than that for Pr = 10^3 under otherwise equal conditions. Further, thermal measurements on weak polymer solutions are accompanied by low values of Pr, and k_1 has the meaning of additional thermal resistance around the transfer surface for a thermal transducer, so one supposes that one possible cause of the reduced sensitivity found in some cases in polymer solutions may be coating of the surface by the polymer.

A difference from a thermoanemometer is that the sensitivity of an anemometer remains reasonably high even for concentrated polymer solutions [12].

The electrodiffusion anemometer has been used in turbulent flows of polymer solutions showing viscoelasticity, and it has been found not always desirable to use a transducer in which the sensitive surface is a continuous cone or wedge. The best design is a wedge with the sensitive component behind the point of incidence. Table 1 gives the basic parameters of the sensors, which differed in dimensions of the sensing element

TABLE 1. Dimensions of Wedge Transducers, mm

Transducer number	1	2	3
Distance of electrode from leading edge	0,50	0,93	0,35
Width of electrode along the flow	0,036	0,071	0,178
Length of electrode transverse to flow	0,54	0,57	0,57
Width of wedge	1,40	1,15	1,25

and distance from the point of incidence. We also used conical transducer No. 4, which had a continuous sensitive element at the vertex of a cone having a generator of length 0.7 mm.

The static and dynamic characteristics of the transducers with displaced sensitive elements may be derived from (2) with the boundary conditions

$$c(x,\ 0) = 0; \quad c(x,\ \infty) = c_0 \tag{4}$$

with the origin of the coordinate system placed at the start of the sensitive element.

As usual, we assume a linear velocity distribution $u = \beta y$ within the diffusion layer for $Pr \gg 1$; as the reacting surface lies to the rear of the point at which the boundary layer arises, and the length of the sensing part along the flow is small, we can use previous assumptions [13, 14] and put $\beta = \text{const}$ as the average value along the electrode. In the general case of the power law of (1), β is to be found by solving the dynamic problem [15]. For example, for a wedge surface

$$\beta = F''(0)\left(\frac{2mn - m + 1}{n+1}\,\frac{\rho b^{2-n}}{k}\right)^{1/1+n} b^{\frac{3}{n+1}}\,\bar{x}^{\frac{3m-1}{n+1}}. \tag{5}$$

Then (2) and (4) are readily solved by introducing the variable

$$\eta = y\left(\frac{\beta_{av}}{Dx}\right)^{1/3}. \tag{6}$$

The total mass flow to the surface is

$$I = \frac{3}{2}\,\frac{c_0 D^{2/3}\beta_{av}^{1/3}}{1.84}\,hL^{2/3}. \tag{7}$$

The dynamic characteristics of this type of device can be determined by solving the following linear differential equation with the above assumptions [13, 14]:

$$\frac{\partial c}{\partial t} + u\frac{\partial c}{\partial x} = D\frac{\partial^2 c}{\partial y^2}, \quad c(x,\ 0,\ t) = 0, \quad c(0,\ y,\ t) = c(x,\ \infty,\ t) = c_0, \tag{8}$$

subject to the condition that the velocity distribution (input signal) varies harmonically. As previously, we assume for $Pr \gg 1$ that the velocity profile is linear: $u/U_0 = \beta y$. To define β we solve the equation

$$\frac{\partial u}{\partial t} + u\frac{\partial u}{\partial \bar{x}} + v\frac{\partial u}{\partial y} = \frac{\partial U}{\partial t} + U\frac{\partial U}{\partial \bar{x}} + \frac{k}{\rho}\,n\left|\frac{\partial u}{\partial y}\right|^{n-1}\frac{\partial^2 u}{\partial y^2}, \tag{9}$$

$$u = v = 0 \quad \text{for} \quad y = 0; \quad u = U(\bar{x},\ t) \quad \text{for} \quad y \to \infty,$$

where

$$U = U_0(1 + \varepsilon\exp(i\omega t)) = U_0 + U_1;\ U_0 = b\bar{x}^m, \quad \varepsilon = \text{const} \ll 1. \tag{10}$$

The solution is defined in the usual way as

$$u = u_0(\bar{x},\ y) + \varepsilon u_1(\bar{x},\ y)\exp(i\omega t), \quad v = v_0(\bar{x},\ y) + \varepsilon v_1(\bar{x},\ y)\exp(i\omega t). \tag{11}$$

We substitute (11) into (9) to get an equation for the steady-state component, for which the solution is known [15], and an equation for $u_1(\bar{x}, y)$:

$$i\omega u_1 - u_1\frac{\partial u_0}{\partial \bar{x}} + u_0\frac{\partial u_1}{\partial \bar{x}} + v_1\frac{\partial u_0}{\partial y} + v_0\frac{\partial u_1}{\partial y} = i\omega U_0$$

$$+ 2U_0\frac{dU_0}{d\bar{x}} + \frac{k}{\rho}\,n\left(\frac{\partial u_0}{\partial y}\right)^{n+1}\frac{\partial^2 u_1}{\partial y^2} + \frac{k}{\rho}\,n(n-1)\frac{\partial u_1}{\partial y}\left(\frac{\partial u_0}{\partial y}\right)^{n-2}\frac{\partial^2 u_0}{\partial y^2} + O(\varepsilon^2), \tag{12}$$

$$u_1 = v_1 = 0, \quad y = 0; \quad u = U_0, \quad y \to \infty.$$

For the case of low frequencies we specify the stream function as the series

$$\Psi_1 = U_0\left(\frac{2mn - m + 1}{n+1}\,\frac{b^{2-n}\rho}{k}\right)^{-\frac{1}{1+n}}\bar{x}^{-\frac{2m-mn-1}{n+1}}\sum_{l=0}^{\infty}(i\bar{\omega})^l g_l(\eta), \tag{13}$$

where $\bar{\omega} = \omega/b\bar{x}^{m-1}$ and η is the self-modeling variable in the stationary problem; we substitute (13) into (12) to get a system of equations for the function g_l that may be solved numerically for various m and n. In what follows we are interested in $g_l''(0)$.

It is readily shown that $g_0^*(0) = [3/(n+1)]F''(0)$; then $g_1''(0)$ can be determined with sufficient accuracy by Lighthill's approximate method [16].

For large ω we follow [17] in specifying Ψ_1 as

$$\Psi_1 = U_0 \left(\frac{2mn - m + 1}{n+1} \frac{\rho b^{\frac{3(1-n)}{2}}}{k} \right)^{-1/1+n} (i\omega)^{-1/2} \bar{x}^{\frac{(n-1)(3m-1)}{2(n+1)}} \sum_{l=0}^{\infty} \alpha^l G_l(\zeta);$$

$$\alpha = \left(\frac{b\bar{x}^{m-1}}{i\omega} \right)^{1/2}; \quad \zeta = y(i\omega)^{1/2} \bar{x}^{\frac{(1-n)(3m-1)}{2(n+1)}} \left(\frac{\rho b^{\frac{3(1-n)}{2}}}{k} \right)^{1/1+n}; \quad \eta = \alpha\zeta. \tag{14}$$

For small α and not very large ζ we assume [17] that

$$F(\alpha, \zeta) = \frac{1}{2} F''(0) \alpha^2 \zeta^2.$$

From (12) and (14) we get a system of equations for the G_l that is solved analytically; the expressions for the G_l are cumbersome and therefore are not given.

With regard to the mass transfer, we assume that

$$\frac{u_0}{U_0} = \beta_{av} y; \quad \frac{u_1}{U_0} = \beta_{1\,av} y. \tag{15}$$

The solution to (8) is sought in the form

$$c = c^0 + \varepsilon \frac{u_1}{u_0} \exp(i\omega t) c_1. \tag{16}$$

For c^0 we get an equation whose solution takes the form of (7), while for c_1 we get an equation that put in terms of the dimensionless variables

$$x_1 = \frac{x}{L}; \quad y_1 = y \left(\frac{\beta_{av}}{LD} \right)^{1/3}; \quad \bar{\omega}_1 = \omega \left(\frac{L^2}{\beta_{av}^2 D} \right)^{1/3} \tag{17}$$

results in

$$i\omega_1 c_1 + y_1 \frac{\partial c_1}{\partial x_1} + y_1 \frac{\partial c^0}{\partial x_1} = \frac{\partial^2 c_1}{\partial y_1^2}, \tag{18}$$

$$c_1(x_1\ 0) = c_1(0,\ y_1) = c_1(x_1,\ \infty) = 0.$$

An equation of the form of (18) has been solved [13] for various $\bar{\omega}_1$.

The frequency response of the sensor is defined as

$$W(i\bar{\omega}_1) = \frac{u_1}{u_0} \frac{I_1}{I_0} \Big/ U_1/U_0; \quad I_1 = D \int_0^L \frac{\partial c_1}{\partial y} \Big|_{y=0} dx. \tag{19}$$

The square of the modulus of the frequency response is

$$|W|^2 = (u_1/u_0)^2 |H|^2,$$

where $|H|^2$ is given by (1.69) of [13].

These expressions allow one to calculate the frequency response and, if necessary, to correct spectral data by means of the following relation [18]:

$$S_i = S_u |W|^2. \tag{20}$$

The viability of this device was checked on an immersed-jet system previously described [11]. The i = f(U) calibration curves were determined with the transducers set in the potential core of an axially symmetrical immersed jet, which was a region of shear-free flow with a rectangular distribution for the mean velocity and a minimal level of turbulent fluctuation. The measurements were also performed along the jet axis to give characteristics such as the mean speed and the longitudinal component of the fluctuating velocity,

TABLE 2. Slopes of Calibration Curves

Solution		Transducer number		
		1	2	3
Pure electrolyte		0,425	0,445	0,445
PEO, %	0,05	0,415	0,425	0,390
	0,01	0,340	0,365	0,310
	0,003	0,450	0,390	0,450
Na-CMC	0,05	0,460	0,440	0,470
	0,01	0,460	0,445	0,465
	0,003	0,460	0,435	0,455

as well as the energy spectrum. A load resistor was inserted in the circuit during the fluctuation measurements, which provided a voltage $V = i \cdot Rl$, where i is the instantaneous current. The signal then passed through an amplifier to a three-octave spectrum analyzer type FSP-80 having a passband from 2 to $2 \cdot 10^4$ Hz. The same function was performed by a TOA-111 spectrum analyzer, which was also used as a wide-band amplifier. The experiments were based on an electrolyte of composition 0.025 M $K_4Fe(CN)_6/K_3Fe(CN)_6$ and 0.5 M K_2SO_4. This electrochemical system has various advantages when used with platinum electrodes: the limiting current corresponds to a wide voltage range, there are no reaction products deposited at the electrodes, the electrochemical reaction is fast, and the system is compatible with water-soluble polymers. Good reproducibility was ensured by using anode – cathode activation. Figure 1b gives calibration curves in the pure electrolyte and in PEO solutions, as well as curves calculated for water from (7). This agreement between theory and experiment is satisfactory. The largest discrepancies occur for transducer No. 3 and are probably due to the size and disposition, since the condition β = const assumed in solving (2) is met less accurately.

The least discrepancy between the calibration curves was observed for the pure electrolyte and a 0.003% PEO solution. The increased velocity of a 0.05% PEO solution caused the calibration curves to lie lower. Figure 1c shows calibration curves for the transducers in Na-CMC solution. The viscosity of an Na-CMC solution differs from that of a PEO solution of the same concentration in that the viscosity is very much closer to that of the pure electrolyte. The slopes of the calibration curves are given in Table 2, and they imply that there is virtually no spread in the slope for Na-CMC, in contrast to PEO. This is probably due to the more

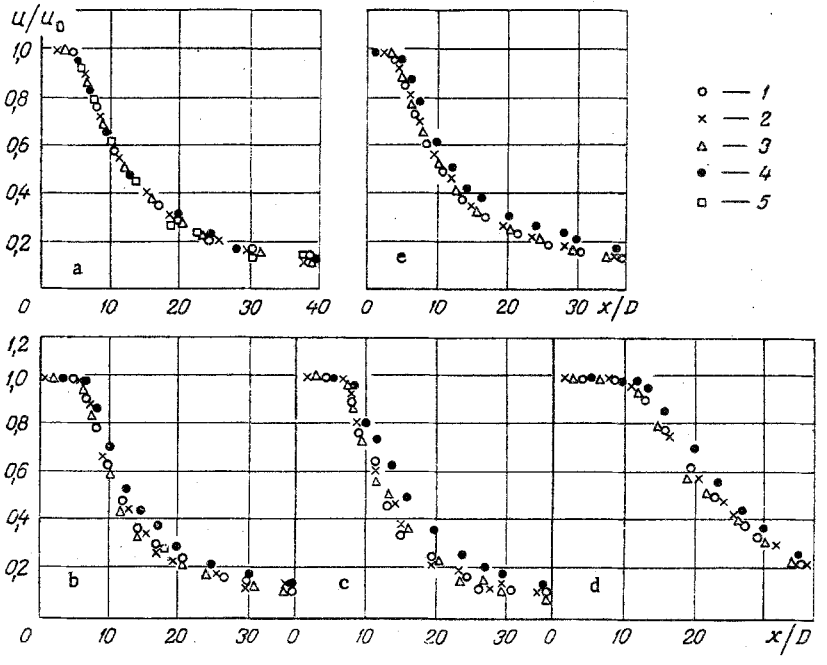

Fig. 2. Measurements of the average axial velocity of an immersed jet with the following transducers: 1) No. 1; 2) No. 2; 3) No. 3; 4) No. 4; 5) Pitot tube; a) pure electrolyte; b-d) PEO solutions with concentrations of 0.003, 0.01, and 0.05%, respectively; e) 0.05% Na-CMC solution.

marked non-Newtonian behavior of PEO solutions. Also, the readouts in the various solutions were stable over long periods. The calibration results indicate that the readout in a dilute polymer solution hardly varies down to the point where the sensitivity is lost at low velocities, in contrast to the marked changes shown with a thermoanemometer.

The calibration curves for the polymer solutions show that the error of measurement is least if the sensitive element is displaced from the point of incidence and the measurements are made in a polymer solution homogeneous in concentration. The relative error of measurement is then only 5-7%. This error may rise to 15-17% for PEO or 9-12% for Na-CMC if the concentration is inhomogeneous.

An axisymmetrical enclosed turbulent jet provides a good means of metrological evaluation for various types of velocity gauge. Figure 2a shows results obtained with a Pitot tube and the electrodiffusion transducers for the distribution of the mean velocity along the axis of a jet of pure electrolyte. The good agreement indicates that the differences in shape and size of the transducers are not decisive for the solvent free from polymer. Parts b-d of Fig. 2 illustrate the effects of PEO on the operation when there is developed turbulent flow. Results obtained with transducers Nos. 1-3 are essentially fitted by a single curve, whose behavior is substantially dependent on the PEO concentration. The length of the initial part increases with the concentration (from 4 diameters at c = 0% to 10 at c = 0.05% PEO), and the jet becomes of long-range type, which is in good agreement with measurements made with a Pitot tube and a laser anemometer [4, 7].

The results obtained with the conical transducer having a continuous sensing element lie somewhat above those for the other transducers, which was also observed with Na-CMC solutions (Fig. 2e). In the range 0.03-0.05% Na-CMC there was a reduction in the range of the jet with transducers Nos. 1-3 and some shortening of the initial segment.

The lag in the transducer may have a marked effect on measurements of the longitudinal component of the velocity fluctuation. For example, Fig. 3 shows data obtained with transducer No. 3, which lie below the curve representing the measurements with transducers Nos. 1 and 2, which are in good agreement with published values. The electrodiffusion anemometer provides information on flow regions where Pitot tubes are of limited use on account of the loss of sensitivity at low flow speeds. This applies particularly to differences in the turbulence at large distances from the nozzle ($x/D > 20$) for immersed jets of water and polymer solutions. Figure 3 shows results obtained with a fast transducer in 0.003% PEO solution, and it is clear that the turbulence at $x/D > 20$ is less than that for water. The available published evidence relates to $x/D < 20$.

Differences in lag can also have a substantial effect in measurements on the spectral density of the velocity fluctuations. Figure 4 shows spectra recorded with the slow transducer No. 3 and a fast transducer ($|W| \sim 1$) (curves 1 and 3). Curve 2 of Fig. 4 shows that there is scope for correcting the spectra from a slow transducer by means of (19) and (20).

The large spread in the results at low frequencies is due to the restricted scope for averaging with the TOA-111 rms voltmeter.

Figure 5 shows the spectral density of the longitudinal component of the velocity fluctuation for $x/D = 20$ as recorded with a fast electrodiffusion transducer, which agrees well with a Pitot tube fitted with a piezoelectric

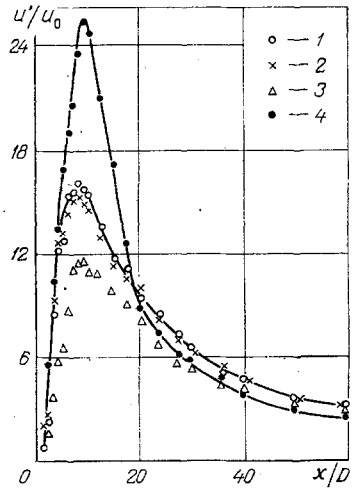

Fig. 3. Variation in turbulence for u'/u_0, %, along the axis of an immersed jet of pure electrolyte (1-3) and of a 0.003% solution of PEO (4) for transducers: 1) No. 1; 2) No. 2; 3) No. 3; 4) No. 1.

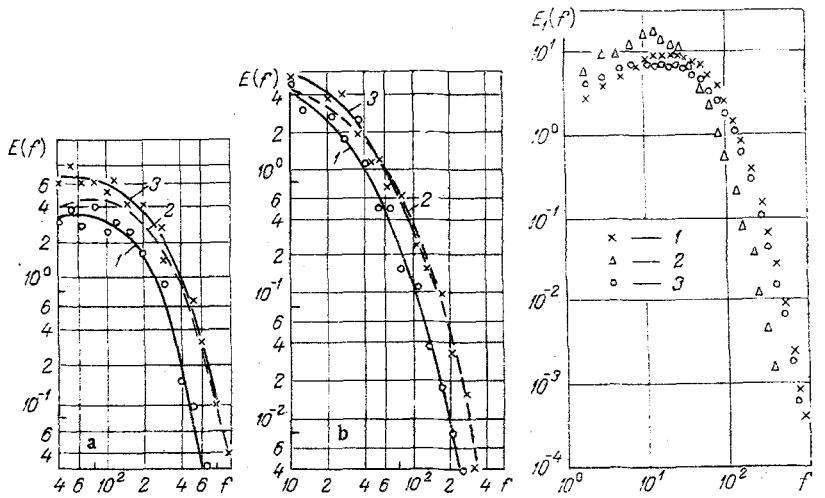

Fig. 4 Fig. 5

Fig. 4. Energy spectra for the longitudinal component of the velocity fluctuation at the axis of a turbulent immersed jet [a) x/d = 10; b) 30]; 1) data recorded with transducer No. 3; 2) data of 1 corrected from (19) and (20); 3) results obtained with a fast transducer. f in Hz.

Fig. 5. Energy spectra for the longitudinal component of the velocity fluctuation at the axis of a jet: 1) pure electrolyte; 2) 0.05% PEO solution; 3) 0.05% Na-CMC solution. $E_i(f)$ in $cm^2 \cdot sec^{-1}$.

transducer [7]. It also shows measurements made in PEO and Na-CMC solutions. There is particularly strong suppression of the high-frequency fluctuations (about 20 dB) in PEO solutions.

In conclusion, we note that the electrodiffusion anemometer is not restricted to specially prepared electrolyte solutions, since the oxygen naturally present in water can be used as an electrochemically active substance that provides the limiting diffusion current at the electrode. Also, the oxygen concentration in the working volume can be monitored by measuring the diffusion current in the nonstationary state. Apparatus employing this method can substantially improve the utility of electrodiffusion anemometry.

NOTATION

n, index of non-Newtonian behavior; k, consistency measure; k_i, electrochemical rate constant; $\bar{x}$, x, y, coordinates; t, time; m, parameter in the velocity law for the boundary layer U, $U = b\bar{x}^m$; h, electrode width; L, electrode length; D, diffusion coefficient; c_0, concentration; S_i, spectral density of flow fluctuations; S_u, spectral density of velocity fluctuations; F, stream function.

LITERATURE CITED

1. E. R. Lindgren and J. L. Chao, Phys. Fluids, 10, 3 (1967).
2. G. Astarita and L. Nicodemo, Ind. Eng. Chem., 8, 3 (1969).
3. G. I. Barenblatt, V. N. Kalashnikov, and A. M. Kudin, "A study of the structure of polymer solutions with a thermoanemometer," Prikl. Mekh. Tekh. Fiz., No. 5, 118 (1968).
4. S. A. Vlasov, O. V. Isaeva, and V. N. Kalashnikov, Inzh.-Fiz. Zh., 25, No. 6 (1973).
5. N. A. Pokryvailo, D. A. Prokopchuk, and Z. P. Shul'man, Inzh.-Fiz. Zh., 29, No. 6 (1975).
6. C. S. Wells and Meyer W. A. Harkness, AJAA, No. 2 (1968).
7. Z. P. Shul'man, N. A. Pokryvailo, N. D. Kovalevskaya, and V. V. Kulebyakin, Inzh.-Fiz. Zh., 25, No. 6 (1973).
8. N. A. Pokryvailo, L. A. Nesterov, A. S. Sobolevskii, T. V. Yushkina, and Yu. E. Zverkhovskii, in: Heat and Mass Transfer V [in Russian], Vol. 10, Minsk (1976).
9. N. A. Pokryvailo and Yu. E. Zverkhovskii, in: Rheophysical Researches [in Russian], Z. P. Shul'man (editor), ITMO AN BSSR, Minsk (1974).
10. Z. P. Shul'man, N. A. Pokryvailo, and T. V. Yushkina, Inzh.-Fiz. Zh., 30, No. 1 (1976).
11. Z. P. Shul'man, N. A. Pokryvailo, A. S. Sobolevskii, and T. V. Yushkina, Inzh.-Fiz. Zh., 30, No. 3 (1976).

12. A. S. Sobolevskii, in: Rheophysics [in Russian], Minsk (1977).
13. S. S. Kutateladze (editor), Research on Turbulent Flows in Two-Phase Media [in Russian], Novosibirsk, Institute Teplofiziki Sib. Otd. Akad. Nauk SSSR (1973).
14. J. P. Reiss and F. J. Hanratty, AJChE J., No. 9, 154 (1963).
15. Z. P. Shul'man and B. M. Berkovskii, The Boundary Layer in a Non-Newtonian Liquid [in Russian], Nauka i Tekhnika, Minsk (1966).
16. M. J. Lighthill, Proc. R. Soc., 224A, 1 (1954).
17. C. R. Ilingworth, J. Fluid Mech., No. 3, 471 (1958).
18. A. A. Sveshnikov, Applied Methods in the Theory of Random Functions [in Russian], Sudpromgiz (1961).
19. Yu. E. Bogolyubov, P. I. Geshev, A. E. Nakoryakov, and I. A. Ogorodnikov, Prikl. Mekh. Tekh. Fiz., No. 4, 113 (1972).

A PHENOMENOLOGICAL DESCRIPTION OF DIFFUSION PROCESSES IN NONIDEAL GASES

P. P. Bezverkhii, V. G. Martynets, and E. V. Matizen

UDC 532.72.533.27

A phenomenological approach to the diffusion problem is presented which allows one to determine the behavior of the coefficient of interdiffusion in nonideal binary gaseous solutions in a rather wide region of variation of the parameters.

The theory of diffusion in dense nonideal gases still remains underdeveloped. In this connection a phenomenological approach to the diffusion problem is offered which permits a satisfactory description of the behavior of the coefficient of interdiffusion near the critical region of vaporization of binary solutions except for a small vicinity of the critical point. This approach is based on propositions of nonequilibrium thermodynamics, and its success is due to the experimentally established relationship consisting in the fact that the mobility of particles in dense gases depends smoothly on the parameters of the system and, in a number of cases, is subject to calculation or experimental determination. Thus, in the given approach principal attention is paid to the analysis of the thermodynamic force – the gradient of the chemical potential. One can be sure that a successful explanation of some of the observed dependences of the coefficient of diffusion on the parameters of the system through such an approach will promote the more intensive development of experiment in this field.

According to nonequilibrium thermodynamics, in a one-phase, two-component system without external fields, with P = const and T = const,

$$j_2 = -L_{12}\frac{\nabla\mu_2}{T} = -nD_{12}\nabla c, \quad j_2 = -j_1, \tag{1}$$

where the fluxes of the components are treated in a relative coordinate system moving with the numerical-mean velocity, and hence D_{12} is treated in the same coordinate system.

One can show [1] that

$$D_{12} = bc(1-c)\left(\frac{\partial\mu}{\partial c}\right)_{P,T}. \tag{2}$$

The mobility entering into Eq. (2) must be distinguished from molecular mobility. They coincide if the concentration approaches zero. Henceforth we have the latter case in mind. It is seen from (2) that the coefficient of interdiffusion depends on the mobility and the derivative of the chemical potential with respect to the concentration. First let us consider the mobility and cite experimental data allowing us to make an assumption about the weakness of its variation. In Fig. 1 we present data on self-diffusion in different gases in a wide range of

Institute of Inorganic Chemistry, Siberian Branch, Academy of Sciences of the USSR, Novosibirsk.
Translated from Inzhenerno-Fizicheskii Zhurnal, Vol. 37, No. 2, pp. 299-306, August, 1979. Original article submitted July 5, 1978.

0022-0841/79/3702-0950$07.50